Sea Surface Thermo- Haline and Subsurface Thermal Structure Variabilities in the South Western Tropical Pacific Ocean during 1979–1985

Thierry Delcroix [1] and Christian Henin[1]

Absteact —Major features of the South Western Tropical Pacific are brought to light through analysis of sea surface salinity samples (23000) and temperature profiles (8500) gathered to study the 1979–1985 period. It is shown that the surface and subsurface oceanic variability is schematically dominated both by the seasonal cycle and the strong 1982–1983 ENSO signal. Specific mechanisms responsible for the ENSO impact upon a) the vertical thermal structure and its related parameters, b) the sea surface temperature, and c) the sea surface salinity are identified and tested.

I. Introduction

In the framework of Air- Sea Interaction studies which are relevant to both the present TOGA and future COARE programs, the South Western Tropical Pacific (SWTP) is an interesting place to focus on. Indeed, the SWTP, defined here between 160 ° E–140 ° W and 24 ° S–10 ° S (Fig.1), is a pertinent region to study since:

a) it is under the influence of the South Pacific Convergence Zone (SPCZ) and of its related wind stress, precipitation regime and convective activity variabilities,

b) it partly belongs to the "warm pool" area where Sea Surface Temperature (SST) is over 28 ° C,

c) it is situated in between Tahiti (French Polynesia) and Darwin (Australia) where sea level pressure records define the usual El Nino / Southern Oscillation (ENSO) index, and

d) it presents the advantage of being quite well monitored since 1979 through ship of opportunity programs.

Besides these Air-Sea Interaction Study Conveniences,it is noteworthy that the SWTP which encompassed numerous Islands is rather poorly documented in the literature.

In this note, thanks to the aforementioned ship of opportunity programs, XBT and Sea Surface Salinity (SSS) data are used to assess the main sub- surface and surface SWTP structures. This permit us to describe the mean and 1979–1985 variability of these structures, and to relate this variability to specif-
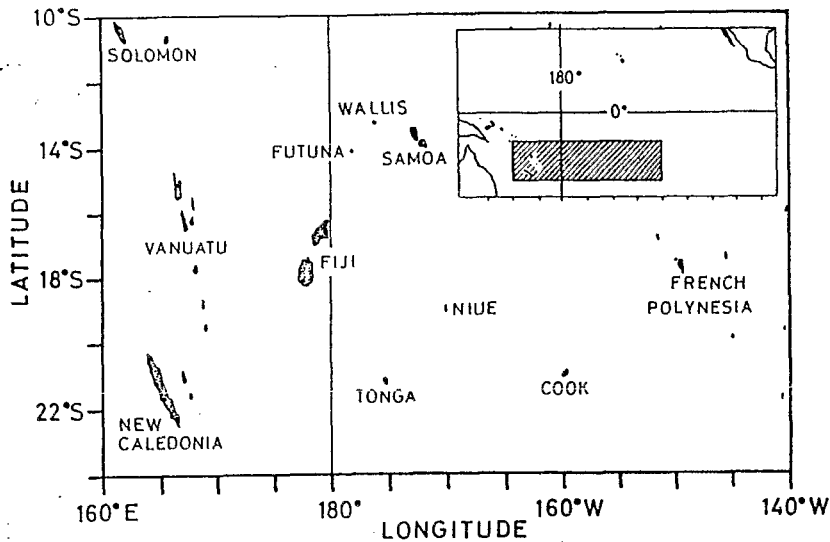

1.Groupe Surtropac Orstom–B.P A5 Noumea–New Caledonia

ic driving mechanisms.

II. The Data

About 23000 SSS samples and 8500 XBT drops have been gathered to study the 1979–1985 period which, interestingly, includes the 1982–1983 ENSO. The spatial distributions of XBT and SSS data (not shown here) are quite homogeneous and both give a comprehensive sampling in longitude-latitude and depth (XBT). The temporal distributions are about 125 XBT. month $^{-1}$ and 300 SSS. month^{-1}. From the raw data, a series of subjective / objective criteria have been carried out in order to detect, correct or delete spurious measurements. Then, the XBT and SSS data were gridded into 2 $^\circ$ latitude, 10 $^\circ$ longitude,1 month and 5 m depth (XBT) grid meshes.

III. The Mean Structures

The mean structures are defined over the 1979–1981 + 1984–1985 years, i.e, excluding the 1982–1983 ENSO period.

A. Sub–Surface

Meridional sections of temperature and of zonal geostrophic currents are shown in Figs 2a–b for the 175 $^\circ$ E longitude.

The temperature section evidences the gradual disappearance of the thermocline, with spreading of the isotherms south of 15 $^\circ$ S. Schematically, the SWTP appears to be a transition zone between typical equatorial and mid-latitude vertical temperature distributions.

The zonal geostrophic velocity section (ref. 400×10^2 hPa) shows a system of eastward and westward currents. South of 15 ° S is the northern part of the large scale anticyclonic gyre; north of 15 ° S is the southern part of the South Equatorial Current (SEC; Wyrtki, 1975).
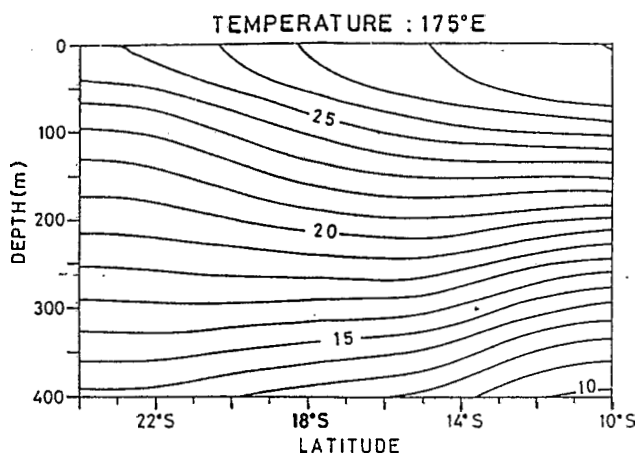

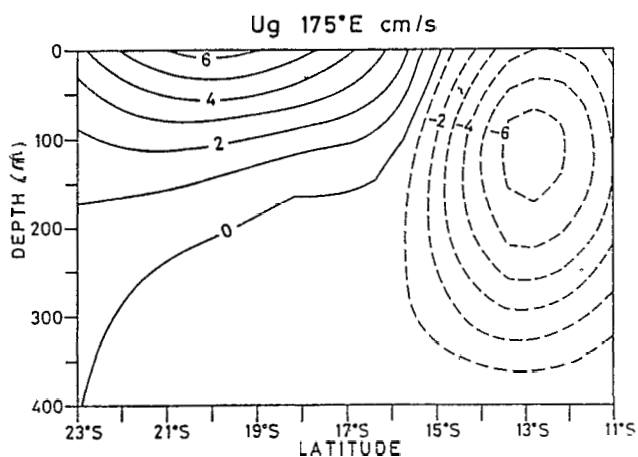**Fig.2 a.** Mean (1979 1981+1984–1985) temperature section at 175   E longitude

Fig.2b. Mean (1979–1981+1984–1985) zonal geostrophic velocity section (ref. 400×10^2 hPa) at 175 ° E longitude

B. Surface

The mean SST map (Fig.2c) shows zonally oriented isotherms ranging from 25 ° C to 29 ° C. North of 15 ° S is the southern part of the equatorial Pacific warm pool (SST > 28 ° C), which migrates to about 12 ° S and 20 ° S during austral winter and summer, respectively.

The mean SSS map (Fig.2d) exhibits an almost SE / NW gradient between the high salinity waters (S > 35.9) of the central south tropical Pacific and the

low ones (S < 34.8) south of the Solomon Islands. Minimum SSS coincides with evaporation minus precipitation (E–p) minimum (Weare et al., 1981) where rainfall can reach as much as 5 m. year^{-1}(Taylor, 1973).
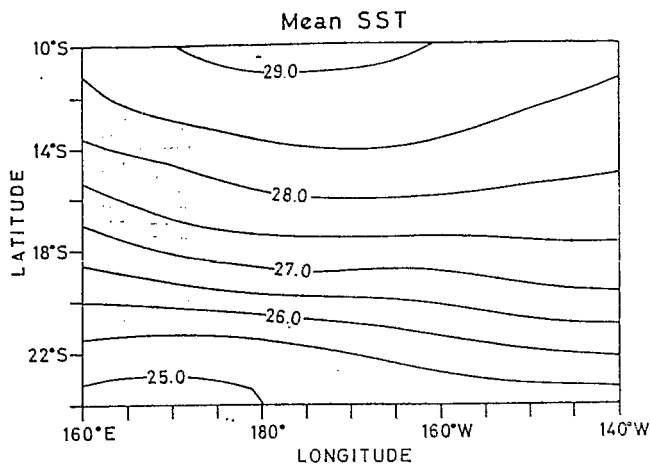
Mean SST

Fig.2c. Mean (1979–1981+1984–1985) sea surface temperature (° C)
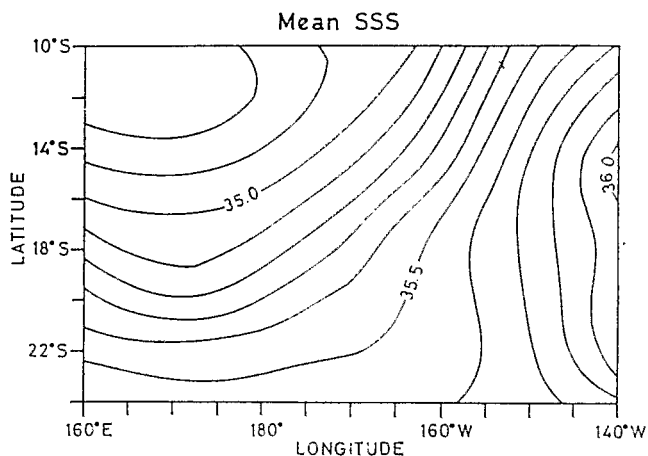
Mean SSS

Fig.2d. Mean (1979–1981 + 1984–1985) sea surface salinity

IV. The Variability During 1979–1985

A. Sub–Surface

The 1979–1985 sub-surface changes are described here through analysis of the average temperature of the 0–400 m layer (hereafter referred to as heat content), and of zonal geostrophic transport computed at 175 ° E longitude.

The first EOF on heat content (FIg.3) accounts for 43% of the variance. The corresponding time function may be decomposed into: a) an accumulation of warm water from mid-1981 to March 1982, b) a net release of heat between April 1982 and May 1983, which constitutes the strong ENSO signal, and c) a return to "normal" situation only reached by 1984. The space function points out that the ENSO signal is mostly restricted north of 15 ° S.
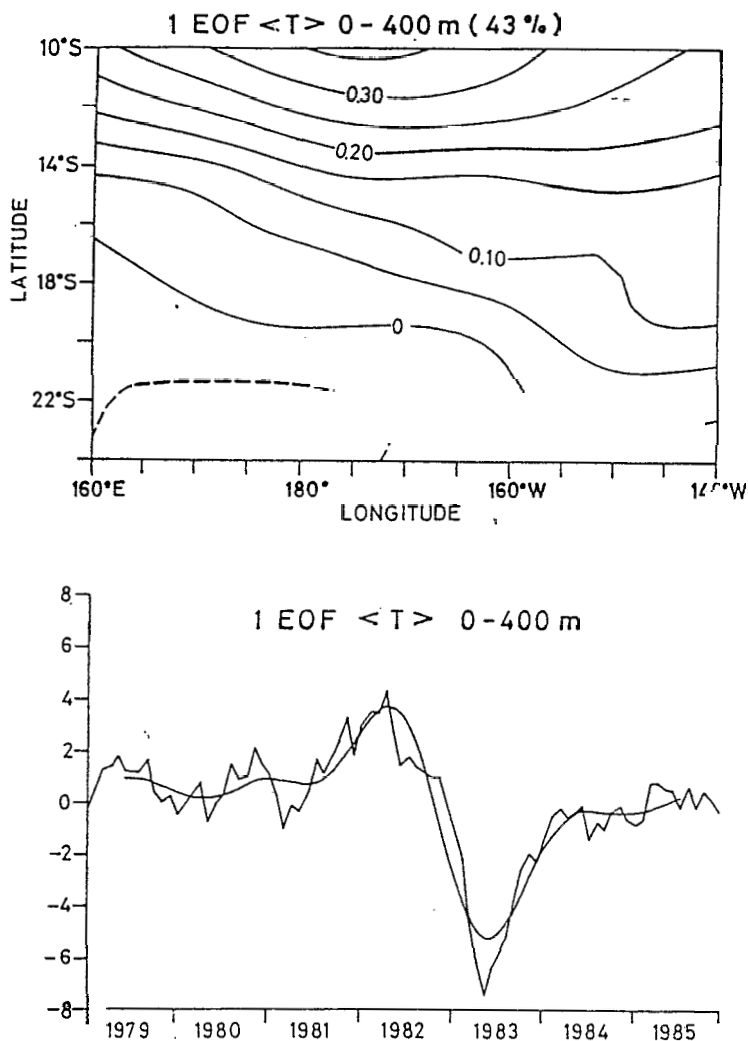

Fig.3. First EOF on the 0–400 m average temperature with spatial pattern (TOP) and time function (BOTTOM). The low frequency curve in the bottom panel is the result of a Fourier low pass filter removing period < 14 months

The 1979–1985 time series of eastward and westward geostrophic transports (175 ° E) are shown in Fig. 4a. The strongest variations occur during the 1982–1983 period when transports are opposed in phase. Inspection of monthly meridional temperature sections (not shown here) evidences that these varia-

144

tions result from an upward movement of isotherms in the northern SWTP. This movement accentuates the meridional temperature gradient (i. e the zonal geostrophic velocity), and displaces southward the center of the subtropical gyre (i. e the surface occupied by westward geostrophic velocities), as exemplified in Fig.4b.
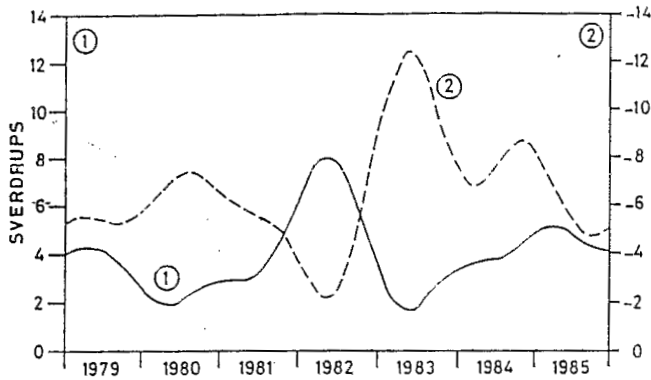

Fig.4a. 1979–1985 time series of eastward (1) and westward (2) geostrophic current transport integrated over 23 ° S–11 ° S at 175 ° E longitude
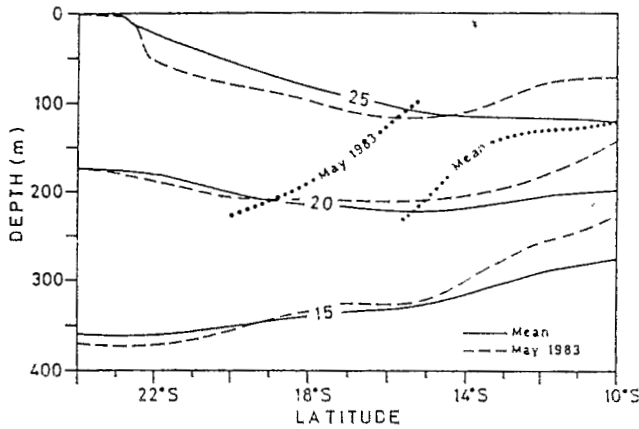
Fig.4b. Latitude-depth diagram of selected isotherm dephts at 175 ° E longitude, during the mean (1979–1981+1984–1985) and May 1983 periods. The dotted lines denote the subtropical gyre center relative to these periods

B.Surface

The first EOF on SST (Fig.5) accounts for 82% of the variance and primarily represents the seasonal cycle with minimum SST in August (austral winter). The interannual variability is depicted by the low frequency curve and evidences that SST reaches maximum cooling at the end of 1982 and early 1983.

SST: 1 EOF (82%)

SST : 1 EOF
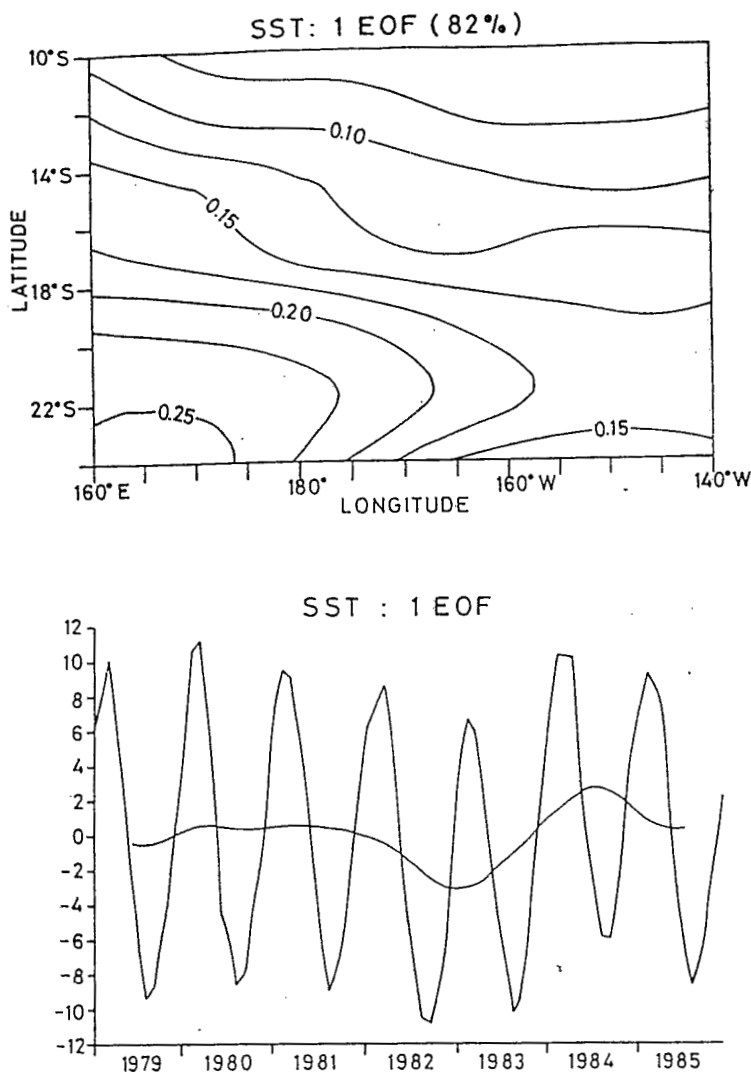
Fig.5. First EOF on SST with spatial pattern (TOP) and time function (BOTTOM). The low frequency curve in the bottom panel as in **Fig.3**

The first EOF on SSS (Fig.6) accounts for 46% of the variance. The pattern of the eigenvector (space function) is maximum along a SE / NW axis representative of the mean SPCZ location. The time function depicts both the seasonal cycle during the "normal" 1979–1981 + 1984–1985 years (minimum in March), and interannual variability associated with the 1982–1983 ENSO phenomenon.

V. Tentative Explanatory Mechanisms

What were the mechanisms responsible for the observed thermal sub-surface and thermo-haline surface changes?

A. Sub-Surface Changes

In extra equatorial region, the simplest dynamical mechanisms that can affect

146

the thermocline depth (thus, heat content and possibly geostrophic transport) is Ekman pumping. The Ekman pumping balance is written as:

$$-\partial h / \partial t = \mathrm{curl}_z(\tau / \rho.f)$$

which can be decomposed in: (1)

$$-\partial h / \partial t = 1 / \rho.f(\mathrm{curl}_z(\tau) + (\beta.\tau^x / f)) \tag{2}$$

where h is the depth of the thermocline and the other variables state for their usual meaning. It is clear from Eq. (2) that the relative magnitude of the two right hand terms determine the sign of Ekman pumping. A qualitative description of these two terms is therefore presented first.
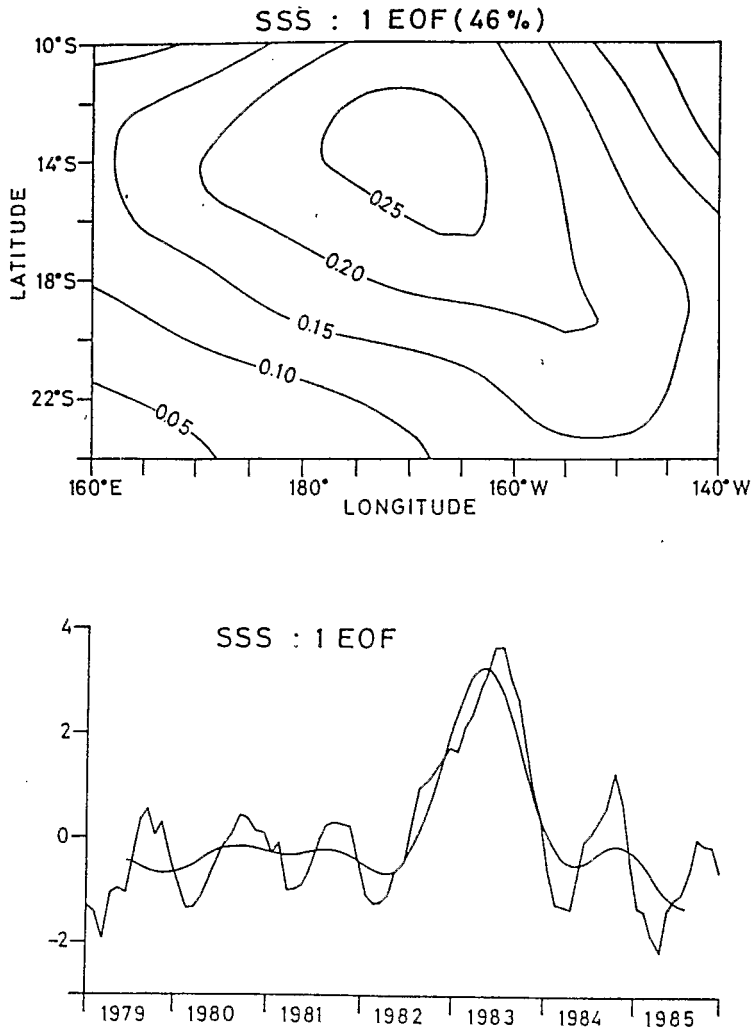

Fig.6. First EOF on SSS with spatial pattern (TOP) and time function (BOTTOM). The low frequency curve in the bottom panel as in **Fig.3**

During a "normal" year, the zonal component of the wind stress (τ^x) is always negative (westward), whereas the seasonal meridional migration of the SPCZ induces alternance of negative and positive (anticyclonic) wind stress curl (curl$_z$&), in the course of the year (Fig.7). Hence, these two terms add or balance, so the SWTP may be sliced into regions:

a) weakly affected by Ekman pumping (east of 170 ° W and south of 13 ° S; south of 20 ° S),

b) favourable to upwelling (west of 170 ° W and north of 13 ° S),

c) favourable to downwelling (east of 170 ° W and north of 13 ° S), and

d) propitious to the alternance of upwelling and downwelling depending of the period of the year (west of 170 ° W and between 13 ° S–19 ° S).
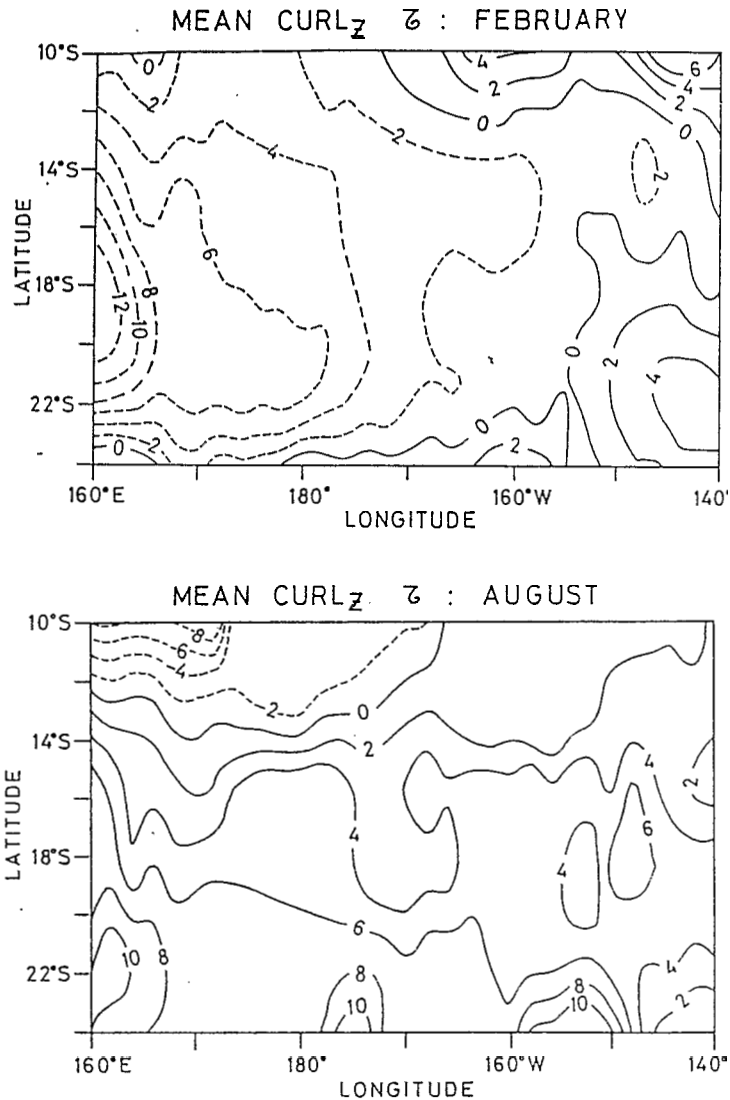
Fig.7. Mean (1979–1981 + 1984–1985) February and August wind stress curls. Contours are at $2.10^{-8} N / m^2$ intervals. The broken lines denote negative values

During the "abnormal" 1982–1983 ENSO period, drastic wind field changes were observed. Of main interest is the reversal of the zonal component of the wind stress (τ^x) in early 1983 between about 13 ° S and the equator, as reported in atlases (e.g Leetmaa and Witte, 1984). At this time, both τ^z and curl τ act in the same way, leading to a strong positive (upward) Ekman pumping velocity in the northern SWTP.

Besides this qualitative approach, a quantitative comparison between the two terms of Eq. (1) has been performed. It is presented in Fig.8 for selected latitudes and longitudes, and enhances the preceeding qualitative discussion . Among features detailed in Delcroix and Henin (1988), the comparison clearly emphasizes the strong 1982–1983 Ekman pumping impact upon the depth of the thermocline (i.e the 20 ° C isotherm depth). To set this impact, it should be realized that the thermocline can shoal to as much as 70 m in May 1983 (11 ° S). Remarkably, local Ekman pumping is thus the main mechanism responsible for the very unusal 1982–1983 upward isotherm movements in the northern SWTP, as well as for the related heat content and zonal geostrophic transport changes, as described above.
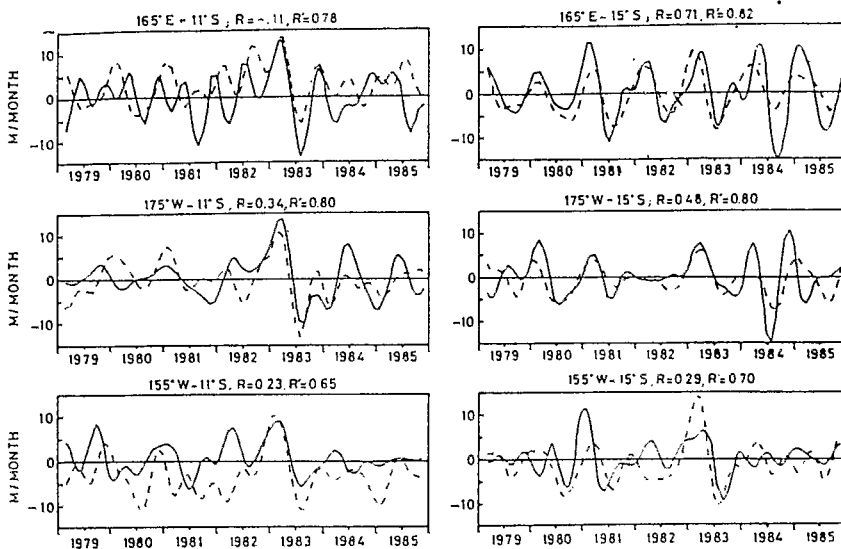

Fig.8. 1979 1985 times series of the two terms of the Ekman pumping balance (see Eq 1). Solid line is $-\partial h / \partial t$, broken line is curl $\tau / \rho f$. R and R' are the correlation coefficients between the 2 terms during the 1979–1981 + 1984–1985 and 1982–1983 periods, respectively

B. Surface Changes

Sea Surface Temperature

The seasonal SST variations (Fig.5) are likely due to the net surface heat flux associated to the seasonal variations of the sun position (Stevenson and Niiler, 1982). Much more intruiguing are the interannual SST variations, i.e the nega-

tive anomalies observed in early 1983 (Fig.5; low frequency curve). Relevant to the COARE objectives, tentative explanations for these variations are proposed here.

In the northern SWTP (10 ° S–15 ° S), the mechanism responsible for SST cooling is Ekman pumping which, as detailed in the previous section, strongly uplifts the thermocline. So, the early 1983 SST cooling anomalies just reflect the underlying thermal structure changes. This is illustrated in Fig.9 which shows the 1979–1985 time series of isotherm depth in a northern 2 ° by 10 ° SWTP box. There, it appears that Ekman pumping modifies the whole water column, as deep as 400m, and clearly disturbs both the normal seasonal cycle and the usually quite constant SST.

In the southern SWTP (15 ° S–24 ° S),variations in latent heat flux are probably the dominant mechanism for producing the discussed SST anomalies. To check this hypothesis, latent heat fluxes have been estimated (Philander et al.'s bulk formulae,1988) over the SWTP during the 1979–1985, owing to available ship reports. The zonal mean (160 ° E–140 ° W) latent heat flux anomalies (ref. 1979–1981 + 1984–1985) are presented in Fig.10. The strongest positive pattern ($>20W.m^{-2}$) occurs south of 15 ° S between December 1982 and April
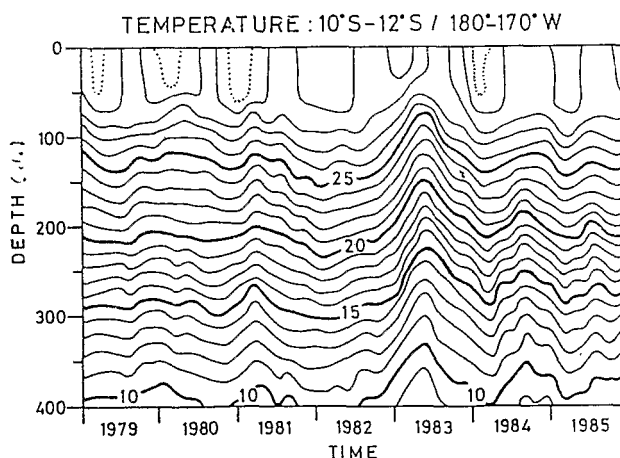
Fig.9. 1979–1985 time series of isotherm depth distributions in the (10 ° S 12 ° S; 180 ° –170 ° W) box

1983. It is both: a) in close timing agreement with the SST anomalies, and b) sufficient to cool a 50m mixed layer by 1 ° C in five months, as observed in the southern SWTP. Hence, despite the uncertainties of latent heat flux calculations, this adds confidence to the role of local evaporation in cooling the western tropical Pacific SST during the 1982–1983 El Nino (Meyers et al., 1986).

Sea Surface Salinity

The seasonal SSS variations (Fig.6) may be due to water advection, evaporation and / or precipitation changes. Only rainfall is examined here. To this end, mean monthly values of SSS are compared with the mean monthly values of *P*

taken from the maps of Taylor (1973). Significant correlations $(R < -0.7)$ are best obtained below the mean SPCZ location (Fig.11), for 2–3 month lags between the twelve month series (i.e, minimum SSS 2–3 months after maximum P). Since P may be reasonably written as $P = PI. \cos(\text{omega. t–theta})$, where omega is the annual frequency and theta is one month (January), the necessary condition for only P governs SSS is satisfied (Hires and Montgomery, 1972). The thickness h of the mixed layer (in density) that would be required to explain that only annual P variations account for annual SSS variations was thus computed over the $R < -0.7$ region. The results show that h should range from extremes of 17 to 44m, with mean values of $28 \pm 7m$. This is in agreement with sparse obsevbations. Therefore, this last comparison together with the phase agreement between SSS and P suggests that, during "normal" year, mostly P governs SSS below the mean SPCZ position.
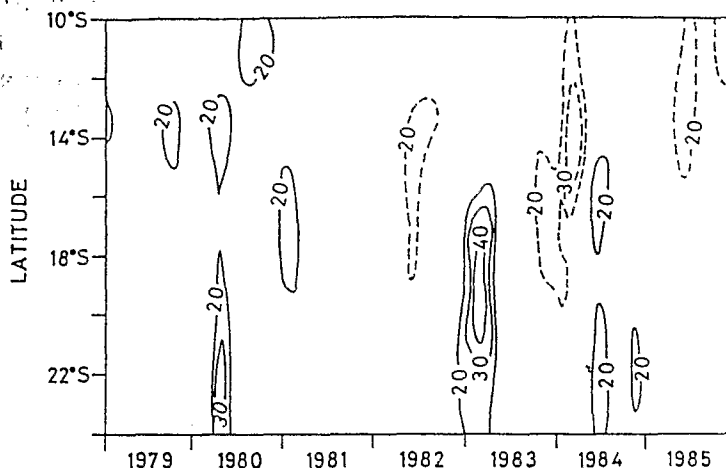

Fig.10. Zonal mean (160 E–140 W) latent heat fluxes anomalies (W m²) with reference the (1979–1981 + 1984–1985) mean year, as a function of time and latitude

The interannual SSS variations (Fig.6), representing the drastic SSS changes associated with the 1982–1983 ENSO, reflects the adding contributions of two different mechanisms. On one hand, the southern branch of the SEC accelerated westward, and extended southward over the SWTP (Fig.4a), bringing water of higher salinity. On the other hand, the SPCZ shifted equatorward, leading to a rainfall deficit below its usual position (Ardanuy et al., 1987; Ropelewski and Halpert, 1987). A rough estimation of both mechanisms allows to evaluate their respective contributions. For example, at 12° S–170° W. the geostrophic advective SSS term $Ug.ds/dx$ is 0.35 per year (mid-1982 to mid-1983), i.e insufficient to account for the observed SSS increase by mid-1983. However, assuming that rainfall linearly decreased from $0.2m.month^{-1}$ in mid-1982 (the mean June value) to 0 in mid-1983 (Ardanuy et al., 1987), we obtain a −1.2m fresh water deficit over a one year period. Alone, such deficit would induce a 0.8 SSS rise over a 50m mixed layer, i.e the same order of magnitude as observed by mid-1983. Rainfall deficit thus appears to be the dominant factor in-

fluencing SSS during the 1982-1983 period.
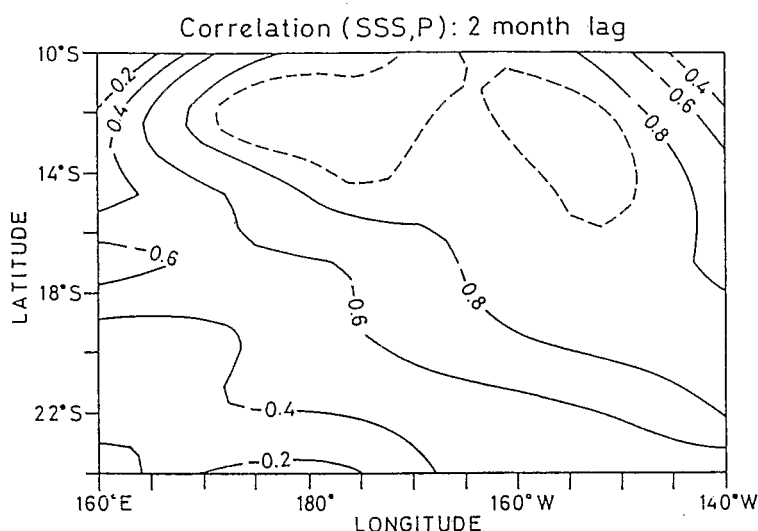
Fig.11. Correlation coefficients between SSS and precipitation mean years for a 2 mouth lag. Contours intervals at 0.2 except for the broken line which denotes the −0.9 value

References

Ardanuy P, P Cuddapah, H Lee Kyle (1987) Remote sensing of water vapor convergence, deep convection and precipitation over the tropical Pacific ocean during 1982–1983 El Nino. J Geophys Res, 92, 14204–14216

Delcroix T, C Henin (1988) On mechanisms of sea surface thermo-haline and sub-surface thermal structure variabilities in the south western tropical Pacific during 1979–1985. Manuscript in prepatation

Hires R, R Montgomery (1972) Navifacial temperature and salinity along the track from Samoa to Hawaii. J Mar Res, 30, 177–200

Leetmaa A, J Witte (1984) El Nino atlas 1982–1983. Leetmaa and Witte editors, NOAA–AOML, Miami, Florida USA 159 pages

Meyers G, J R Donguy, R K Reed (1986) Evaporative cooling of the western equatorial Pacific by anomalous winds. Nature, vol 323, No 6088, 523–526

Philander S, W Hurlin, A Seigel (1988) Simulation of the seasonal cycle of the tropical Pacific ocean. J Phys Oceanogr, vol 17, 1986–2002

Ropelewski C, M Halpert (1987) Global and regional scale precipitation patterns associated with the El Nino-Southern Oscillation. Mon Wea Rev,115, 1606–1626

Stevenson J, P niiler (1982) Upper ocean heat budget during the Hawaii to Tahiti shuttle experiment. J Phys Oceanogr, vol 13, 1894–1907

Taylor R (1973) An atlas of Pacific island rainfall. Hawaii Institute of Geophysics. University of Hawaii, HIG-73-9

Weare B, P Strub, M Samuel (1981) Annual mean surface heat fluxes in the tropical Pacific ocean. J Phys Oceanogr, vol 11, 705–717

Wyrtki K (1975) Fluctuations of the dynamic topography in the Pacific ocean.J Phys Oceanogr, vol 5, 450–459